000000000PE

Mathematical modeling for optimization of competition sailplane flight: a preliminary approach

Paulo Henriques Iscold Andrade de Oliveira
Prof. Ricardo Luiz Utsch de Freitas Pinto
Centro de Estudos Aeronáuticos (*Center for Aeronautics Studies)* of the Engineering School of the Universidade Federal de Minas Gerais (*Federal University of Minas Gerais)* – CEA/EEUFMG

ABSTRACT

In this work, sailplane symmetrical motion equations including pitch motion controlled by elevator angle are presented. The following effects are especially taken into consideration: i) tail damping due to pitch motion; ii) air density variation according to altitude; iii) presence of vertical and horizontal atmospheric air motions, and iv) non-linearity of $C_L \times \alpha$ curve near stall angle. The mathematical modeling includes the construction of an objective function for competition flight optimization. Making use of the concept of state variables, the minimum time trajectory problem is formulated as an optimal control problem with state constraints. Using simplified control laws and a mathematical programming algorithm, sub-optimal trajectories are obtained for the sailplane *PIK-20B*.

INTRODUCTION

The classical optimization problem in sailplane competitions (Weinholtz, 1967, Reichmann, 1978) consists in minimizing time spent in sailplane cruising from one thermal to another and in the rise within the second thermal until it recovers its initial altitude (Figure 1).

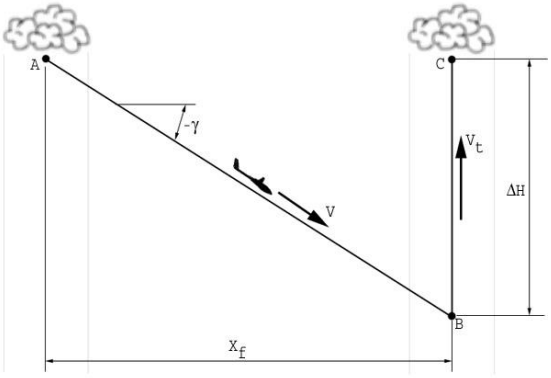

Figure 1 – The MacCready Problem

The MacCready solution, although very efficient in practical conditions, is based on equilibrium analysis and does not take into account the transient dynamics of the problem. Recently, other authors have studied this problem from a dynamic point of view as an optimal control problem (Metzger e Hendrick, 1974; Pierson e De Jong, 1978; Dickmanns, 1981; De Jong, 1981; Mozdyniewicz, 1981; Kawabe e Goto, 1994; Vanderbei, 2000). However, all these studies are based on simplified dynamic models, without taking into account the pitch motion, adopting as the control variable the lift coefficient of the sailplane and not the elevator angle which would be most natural from a practical point of view.

This present approach includes pitch motion and adopts the elevator angle as the control variable, taking into account: i) air density variation with altitude; ii) presence of atmospheric air motion and iii) non-linear behavior of the lift near to the stall.

Limitations in flight altitude and in velocity are modeled as state constraints, which are later incorporated in the objective function through penalties.

Preliminary results are obtained using the sailplane *PIK-20B* data.

MOTION EQUATIONS

The force diagram used to determine motion equations for a sailplane in symmetrical flight, including pitch motion, is presented in Figure 2.

The main considerations for the construction of this diagram are:

1) the contribution of drag forces for pitch motion is very small;
2) while lift forces for the wing and fuselage are grouped (L), horizontal tail lift is considered separately (L_T);

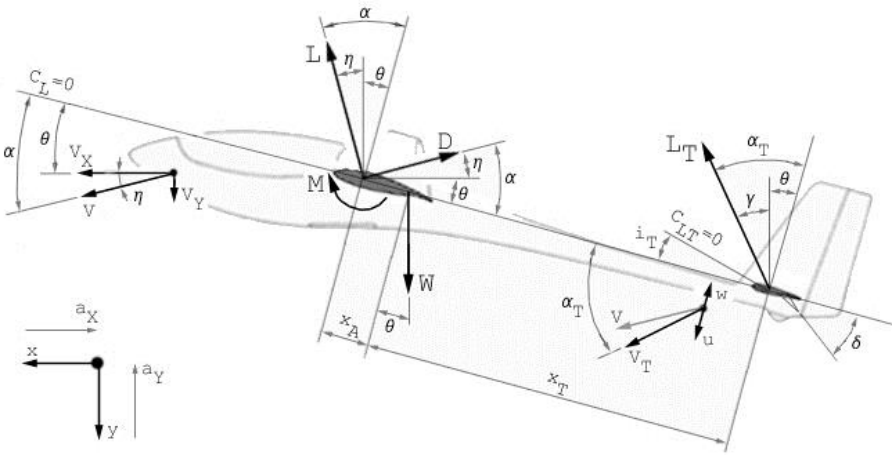

Figure 2 – Force Diagram

3) the effect of the horizontal tail aerodynamic moment around its aerodynamic center on sailplane pitch motion is negligible. Therefore, the aerodynamic moment (*M*) refers only to the aerodynamic moment of the wing-fuselage group around its aerodynamic center.

Notice that the diagram includes the presence of vertical and horizontal atmospheric air motions (a_X e a_Y), which may vary in intensity throughout space.

An inertial system is adopted as reference and its origin is located exactly in the initial position (*t=0*) of the sailplane gravity center, with its *x* axis positioned in the local horizontal, pointed towards the initial direction of motion and its *y* axis positioned on the local vertical, pointed downwards.

Therefore, V_X represents the horizontal component of the sailplane inertial velocity and V_Y its vertical component (descending velocity).

Applying Newton's Second Law, the following equations are obtained for the inertial sailplane accelerations:

horizontal direction:

$$m\ddot{x} = L\text{sen}\eta - D\cos\eta + L_T\text{sen}\gamma \qquad (1)$$

vertical direction:

$$m\ddot{y} = -L\cos\eta - D\text{sen}\eta + L_T\cos\gamma + W \qquad (2)$$

pitch motion:

$$J\ddot{\theta} = M + L\cos\alpha \cdot x_A - L_T\cos\alpha_T \cdot x_T \qquad (3)$$

In the above equations, *m* and *J* denote, respectively, the sailplane mass and its inertial moment around the transversal axis. The right hand side of the equations are calculated taking into account the following considerations.

The aircraft aerodynamic velocity modulus can be written as:

$$|V_R| = \sqrt{V_x + a_X}^{\,2} + \sqrt{V_x + a_Y}^{\,2} \qquad (4)$$

where the horizontal atmospheric air velocity (a_X) is positive when the wind is frontal in relation to the initial aircraft position and the vertical atmospheric air velocity (a_Y) is positive for ascending atmospheric air motions. Therefore, the angle between the aircraft aerodynamic velocity and the horizontal (η) can be written as:

$$\eta = \text{arctg}\left[\frac{V_y + a_Y}{V_x + a_X}\right] \qquad (5)$$

The attack angle for the wing-fuselage, related to its non-lift line is:

$$\alpha = \eta + \theta \qquad (6)$$

where θ denotes the angle between the wing-fuselage non-lift line and the horizontal.

In order to calculate the attack angle on the horizontal tail (Figure 3) two parts are taken into account: the first as a consequence of the sailplane attack angle, including the down-wash effect produced by the wing and the second as a consequence of the sailplane pitch motion.

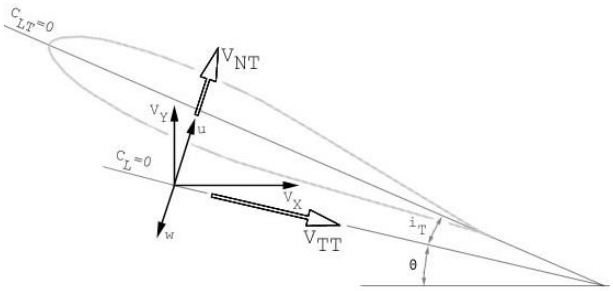

Figure 3 –Velocity components on horizontal tail

The horizontal tail aerodynamic velocity modulus is obtained as:

$$|V_{RT}| = \sqrt{V_{TT}^{\ 2} + V_{NT}^{\ 2}} \tag{7}$$

where V_{NT} and V_{TT} denote the normal and tangential components of horizontal tail aerodynamic velocity related to the wing-fuselage non-lift line, calculated as:

$$V_{TT} = V_X + a_X \cos\theta - V_Y + a_Y \operatorname{sen}\theta \tag{8}$$

$$V_{NT} = V_X + a_X \operatorname{sen}\theta - V_Y + a_Y \cos\theta + u - w \tag{9}$$

with the down-wash (w) and the pitch (u) effects included.

The velocity (u) due to pitch motion is obtained as:

$$u = \theta \cdot x_T \tag{10}$$

where x_T denotes the distance between the horizontal tail and wing-fuselage aerodynamic centers, measured parallel to the wing-fuselage non-lift line.

The velocity (w) due to the down-wash effect is obtained as:

$$w \cong \varepsilon V_R \tag{11}$$

where

$$\varepsilon \cong \alpha \left.\frac{d\varepsilon}{d\alpha}\right|_0 \tag{12}$$

denotes the *down-wash* angle.

The horizontal tail attack angle related to the wing-fuselage non-lift line is:

$$\alpha_T = \operatorname{arctg}\left(\frac{V_{NT}}{V_{TT}}\right) \tag{13}$$

In order to calculate the horizontal tail attack angle related to its non-lift line, the angle between the horizontal tail and wing-fuselage non-lift lines (i_T) must be added to the previous value, as follows:

$$\alpha_T^0 = \alpha_T + i_T \tag{14}$$

The wing-fuselage lift, drag and aerodynamic moment can be written as:

$$L = \tfrac{1}{2}\rho(y) S C_L(\alpha) V_R^2 \tag{15}$$

$$D = \tfrac{1}{2}\rho(y) S C_D(\alpha) V_R^2 \tag{16}$$

$$M = \tfrac{1}{2}\rho(y) S \overline{\overline{c}} C_M(\alpha) V_R^2 \tag{17}$$

where S denotes the wing area, $\overline{\overline{c}}$ denotes the wing mean aerodynamic chord and C_L, C_D, C_M denote the respective coefficients.

The horizontal tail lift can be written as:

$$L_T = \tfrac{1}{2}\rho(y) S_T C_{LT}(\alpha_T, \delta) V_{RT}^2 \tag{18}$$

where S_T denotes the horizontal tail area, δ the elevator angle and C_{LT} the respective coefficient.

STATE EQUATIONS

Taking all the previous considerations into account, a set of state variables can be defined as:

$$\begin{aligned} x_1 &= x \\ x_2 &= y \\ x_3 &= \theta \\ x_4 &= \dot{x} = V_X \\ x_5 &= \dot{y} = V_Y \\ x_6 &= \dot{\theta} = q \end{aligned} \tag{19}$$

In terms of state variables, the sailplane symmetrical motion equations can be written as follows:

$$\begin{aligned} \dot{x}_1 &= x_4 \\ \dot{x}_2 &= x_5 \\ \dot{x}_3 &= x_6 \\ \dot{x}_4 &= \frac{1}{m}\left[L sen\ \eta - D\cos\eta + L_T sen\ \gamma \right] \\ \dot{x}_5 &= \frac{1}{m}\left[-L\cos\eta - D sen\ \eta + L_T \cos\gamma + W \right] \\ \dot{x}_6 &= \frac{1}{J}\left[M + L\cos\alpha \cdot x_A - L_T \cos\alpha_T \cdot x_T \right] \end{aligned} \tag{20}$$

where:

$$L = \tfrac{1}{2}\rho(x_2) S C_L(\alpha) V_R^2$$

$$D = \tfrac{1}{2}\rho(x_2) S C_D(\alpha) V_R^2$$

$$M = \tfrac{1}{2}\rho(x_2) S \overline{\overline{c}} C_M(\alpha) V_R^2$$

$$L_T = \tfrac{1}{2}\rho(x_2) S_T C_{LT}(\alpha_T, \delta) V_{RT}^2$$

$$|V_{RT}| = \sqrt{V_{TT}^{\ 2} + V_{NT}^{\ 2}}$$

$$\gamma = \alpha_T - x_3$$

$$\alpha_T = \tan\left(\frac{V_{NT}}{V_{TT}}\right)$$

$$V_{TT} = x_4 + a_X \cos x_3 - x_5 + a_Y\ sen\ x_3$$

$$V_{NT} = x_4 + a_X\ sen\ x_3 + x_5 + a_Y \cos x_3 + u - w$$

$$w = \alpha V_R \left.\frac{d\varepsilon}{d\alpha}\right|_0$$

$$u = x_6 \cdot x_T$$

$$V_R = \sqrt{x_4 + a_X{}^2 + x_5 + a_Y{}^2}$$

$$\alpha = \eta + x_3$$

$$\eta = \mathrm{arctg}\left[\frac{x_5 + a_Y}{x_4 + a_X}\right]$$

Notice that, in the above state model, the control variable is the elevator angle (δ).

The use of the elevator angle as a control variable is extremely realistic since, indeed, the pilot controls the flight through variations in the stick position, i.e. in the elevator angle.

OPTIMIZATION PROBLEM FORMULATION

The final goal of the present study is to make use of the previous dynamic model in order to solve the MacCready problem (Figure 1), having as control variable the elevator angle, as the following optimal control problem:

$$\min_{\delta} \int_0^{t_f} dt + \int_{x_2}^{x_2} \int_0^{t_f} \frac{dy}{V_T} \qquad (21)$$

subject to:

$$x\ \delta\ < x_f;$$
$$V_T \quad \text{known};$$
$$\mathrm{V}\ \delta\ < VNE;$$
$$x_2\ 0\ - x_2\ t_f\ < h$$

where *VNE* denotes the velocity never to be exceeded, an sailplane operational restriction, *h* denotes the initial height of the trajectory. The second integral in the equation (21) represents the time in the rise within the thermal. The states $x(\delta)$ and $V(\delta)$ must be calculated by numerical integration of state equations. It is also assumed that the limit load factors will never be reached.

In this paper, in order to simplify the problem and enable a preliminary analysis, the problem was solved only regarding the time spent between thermals, i.e. substituting the problem(21), the following optimal control problem must be solved:

$$\min_{\delta} \int_0^{t_f} dt \qquad (22)$$

subject to:

$$x\ \delta\ < x_f;$$
$$V\ \delta\ < VNE$$

Notice that the constraint on height was removed in problem(22). For the moment, it is tacitly admitted that the sailplane initial height is greater than the maximum loss of height during the trajectory.

PENALIZED PROBLEM

Through the Optimal Control Theory arguments (Pinto, 1991), it is possible to manipulate problem (22) in order to rewrite it in the following penalized form:

$$\min_{\delta} \int_0^{t_f} 1 + J\ \ dt \qquad (23)$$

where:

$$J = \begin{cases} 0 & V < VNE \\ V - VNE\ ^2 & V > VNE \end{cases}$$

subject to:

$$x\ \delta\ < x_f$$

Notice that, in problem(23), there is still a formal state inequality constraint that, in fact, must be used only as a stop criterion in the numerical integrations (as final sailplane horizontal displacement).

CONSTRUCTION OF A SUB-OPTIMAL CONTROL PROBLEM

The problem of finding the exact optimal control law for the sailplane trajectory is a hard task to accomplish, mainly due to the complexity of the dynamic model studied.

Therefore, it is appropriate to adopt parametric sub-optimal approximations. These parametric forms for the control law can be specified by a finite number of coefficients, which transform the optimal control problem into a mathematical programming problem (Pinto, 1982).

In the present paper, the sailplane range was divided into finite number of elements over which the sub-optimal control must be constant. Therefore, if the sailplane trajectory is divided into *m* elements, one has *m* parameters to be optimized.

BOUNDARY CONDITIONS

The boundary conditions to be previously specified are:

- The six initial state variables;
- The distance between the thermals, i.e. the desired sailplane range.

The initial state variables were chosen as the sailplane equilibrium conditions at the minimum sink rate velocity. This option was made taking into account that this will be the sailplane velocity during ascending flights in thermals, the condition just before cruising towards the next thermal.

AERODYNAMIC POLAR

To allow for fast and coherent numerical operations, the $C_L \times \alpha$ curve was adopted as a function composed by a straight line segment connected to cubic polynomials in its

extremities. Continuity and smoothness must be preserved over the junction points of the linear and cubic portions. The $C_{L\max}$ value and its corresponding attack angle must be coincident with the original ones. For the drag polar a complete quadratic function was used, as usual.

OPTIMIZATION ALGORITHM

Considering the unconstrained and parametric form of the penalized sub-optimal control problem, the *Fletcher-Reeves* version of *Conjugated Gradient Method* was adopted as an iterative algorithm in order to proceed in the search for the optimal solution (Luenberger, 1984).

NUMERICAL OBJECTIVE FUNCTION EVALUATIONS

For the numerical solutions, the objective function must be evaluated by numerical integration of differential equations. The following fifth order adaptive version of the *Runge-Kutta Method* was adopted (Press et al., 1992):

Numerical Integrator

In order to solve the system of differential equations

$$\dot{y} = f\ \ x, y \tag{24}$$

with initial condition $y\ \ x_0\ \ = y_0$,

use the recursive equation:

$$y_{n+1} = y_n + \sum_{i=1}^{6} c_i k_i \tag{25}$$

where:

$k_1 = hf\ \ x_n, y_n$

$k_2 = hf\ \ x_n + a_2 h, y_n + b_{21} k_1$

$\vdots$

$k_6 = hf\ \ x_n + a_6 h, y_n + b_{61} k_1 + \cdots + b_{65} k_5$

which coefficients are shown in Table 1.

Table 1 – Fifth Order Adaptative Runge-Kutta Coefficients

i	a_i	b_{ij}					c_i
1	-	-	-	-	-	-	$\frac{37}{378}$
2	$\frac{1}{5}$	$\frac{1}{5}$	-	-	-	-	0
3	$\frac{3}{10}$	$\frac{3}{40}$	$\frac{9}{40}$	-	-	-	$\frac{250}{261}$
4	$\frac{3}{5}$	$\frac{3}{10}$	$-\frac{9}{10}$	$\frac{6}{5}$	-	-	$\frac{125}{594}$
5	1	$-\frac{11}{54}$	$\frac{5}{2}$	$-\frac{70}{27}$	$\frac{35}{27}$	-	0
6	$\frac{7}{8}$	$\frac{1631}{55296}$	$\frac{175}{512}$	$\frac{575}{13824}$	$\frac{44275}{110592}$	$\frac{253}{4096}$	$\frac{512}{1771}$
j		1	2	3	4	5	

NUMERICAL DERIVATIVES

One of the greatest hardships in the *Fletcher-Reeves Method* implementation is the evaluation of the objective function partial derivatives. This calculation, due to the complexity of the objective function, must be done through a numerical procedure.

The perturbation techniques have been the most applied practice for the numerical derivatives calculations. A simple procedure is to adopt the expression:

$$f'\ x\ \ = \frac{f\ \ x\ \ - f\ \ x - h}{h} \tag{26}$$

$$f'\ x\ \ = \frac{f\ \ x + h\ \ - f\ \ x}{h} \tag{27}$$

$$f'\ x\ \ = \frac{f\ \ x + h\ \ - f\ \ x - h}{2h} \tag{28}$$

which provides, respectively, the backward, the forward and the centered derivatives.

The use of these expressions is not always satisfactory and their convergence is largely dependent on the behavior of the function. In the present study, since the behavior of the objective function of the problem is not known, one cannot consider that to be a well behaved function. Indeed, it is expected that this function will present an irregular behavior, especially if two effects take place during the trajectory: i) sailplane stall, and ii) velocity limit violation, when penalties will occur.

In order to overcome this difficulty, the derivatives calculation was made through the *Ridders´s Algorithm*, which controls the magnitude of perturbations (Press et al., 1992).

All these previous procedures presented failures around the points where the left and right derivates had opposite signs or very different magnitudes. In order to overcome this problem, the derivatives were evaluated as:

$$f'\ x\ \ = \frac{f\ \ x + h\ \ - f\ \ x - h}{2h} \tag{29}$$

if the derivates to the left and the right have the same sign, and:

$$f'\ x\ \ = 0 \tag{30}$$

if the derivates to the right and the left have opposite signs.

NUMERICAL SOLUTIONS

Taking for an example the sailplane *PIK-20B* (see Figure 4 and Table 2), the initial conditions for the problem are as shown in the expression(31).

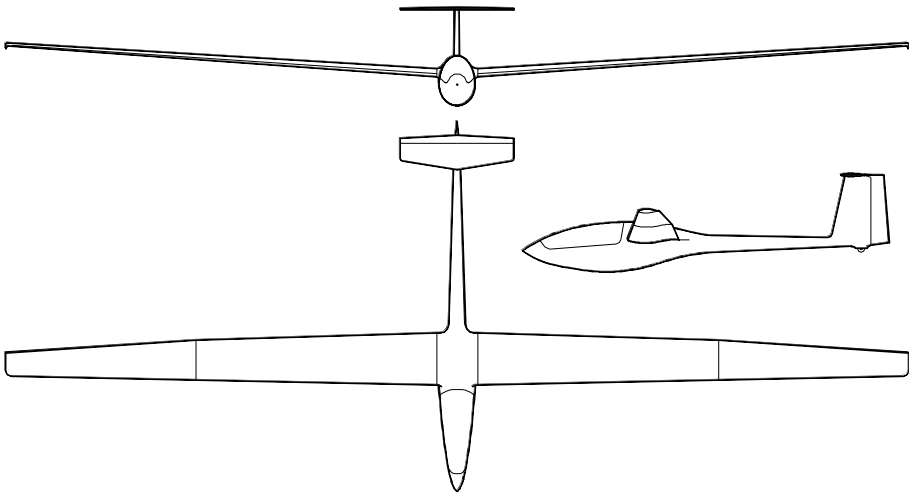

Figure 4 –*PIK-20B* three views

Table 2 –*PIK-20B basic specifications*

Wing Span	15.00 m	**Maximum weight**	450 kgf
Length	6.45 m	**Wing profiles:**	FX67-K-170
Wing area	10.00 m²		FX67-K-150
Aspect Ratio	22.50	**Hor.Tail span**	2.00 m
Empty weight	220 kgf	**Hor.Tail area**	0.975 m²

$$\begin{aligned} x_1 &= 0m \\ x_2 &= 0m \\ x_3 &= 3.2661^\circ \\ x_4 &= 22.2245\, m/s \\ x_5 &= 0.6718\, m/s \\ x_6 &= 0\,^\circ/s \end{aligned} \tag{31}$$

The *PIK-20B* drag polar (Pinto et al., 1999) was adjusted as to following parabolic expression (attack angle in degrees) (Figure 5):

$$\begin{aligned} C_D = \;& 2{,}0907 \times 10^{-4}\;\; \alpha^2 \\ +\;& 1{,}7714 \times 10^{-3}\;\; \alpha \\ +\;& 1{,}6229 \times 10^{-2} \end{aligned} \tag{32}$$

The $C_L \times \alpha$ curve was defined as (Figure 5):

$$\begin{cases} C_L = -0.0017\;\; \alpha + 12\;^3 \\ \quad +0.0228\;\; \alpha + 12\;^2 - 0.4 \end{cases} \quad \alpha < -5.9672^\circ$$
$$C_L = 0.0883\;\; \alpha + 6.5467 \quad -5.9672^\circ < \alpha < 10.9102^\circ \tag{33}$$
$$\begin{cases} C_L = -0.0023\;\; \alpha - 15\;^3 \\ \quad -0.0249\;\; \alpha - 15\;^2 + 1.8 \end{cases} \quad \alpha > 10.9102^\circ$$

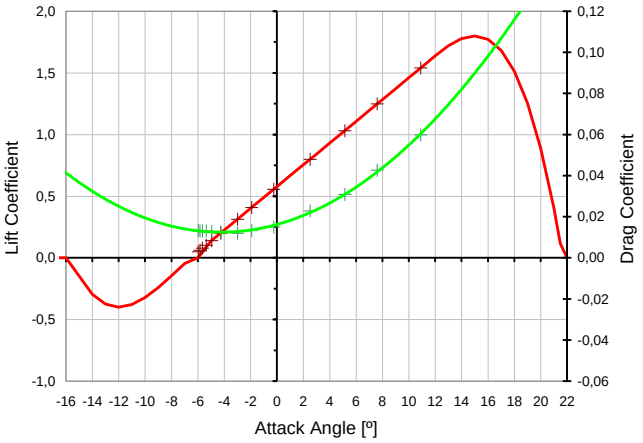

Figure 5 –PIK-20B aerodynamic curves

Optimal results were obtained for three ranges: 1000, 2000, and 4000 *meters*.

Table 3 shows the optimal results for the problem with 1000*m* of range, considering 1, 2, 4, and 8 elements. The sub-optimal trajectories, velocity profiles and control curves, are shown, respectively, at Figure 6, Figure 7, and Figure 8.

Notice that, for the convergence criteria adopted, solutions with 4 and 8 elements are identical.

For the 2000*m* range problem the optimal results obtained for 1, 2, 4, and 8 elements are shown in Table 4, Figure 9, Figure 10, and Figure 11.

Notice that, once again, for the convergence criteria adopted, solutions with 4 and 8 elements are identical.

Similarly, the optimal results obtained for the 4000*m* range problem are shown in Table 5, Figure 12, Figure 13, and Figure 14.

Notice that, in this case, the 4 and 8 elements solutions are significantly different.

Table 3 –1000m range results

DELTA1 (°)	DELTA2 (°)	DELTA3 (°)	DELTA4 (°)	DELTA5 (°)	DELTA6 (°)	DELTA7 (°)	DELTA8 (°)	TIME (SEC)
.1081	-	-	-	-	-	-	-	22.63
.0039	1.1062	-	-	-	-	-	-	21.64
.2082	-.0864	1.0398	1.0825	-	-	-	-	21.53
.2082	.2082	-.0864	-.0864	1.0398	1.0398	1.0825	1.0825	21.53

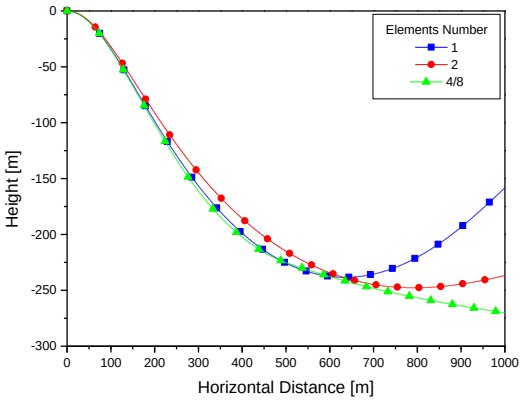

Figure 6 – 1000m range sub-optimal trajectories

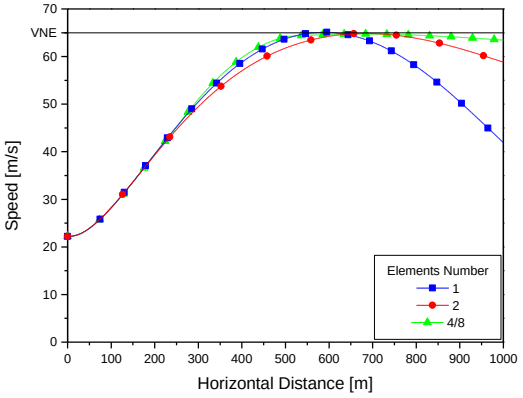

Figure 7 – 1000m range velocity profiles

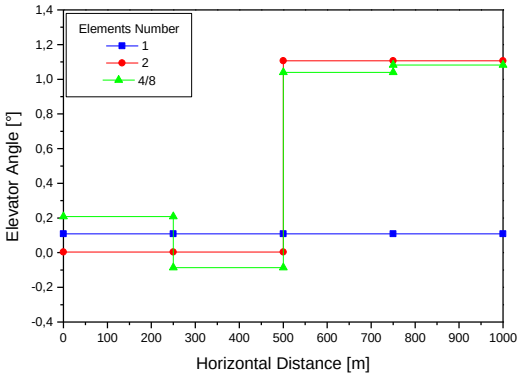

Figure 8 – 1000m range sub-optimal control

Table 4 – 2000m range results

DELTA1 (°)	DELTA2 (°)	DELTA3 (°)	DELTA4 (°)	DELTA5 (°)	DELTA6 (°)	DELTA7 (°)	DELTA8 (°)	TIME (SEC)
.1074	-	-	-	-	-	-	-	46.81
.1032	.5077	-	-	-	-	-	-	45.51
.0195	1.0849	1.2438	1.1024	-	-	-	-	38.22
.0195	.0195	1.0849	1.0849	1.2438	1.2438	1.1024	1.1024	38.22

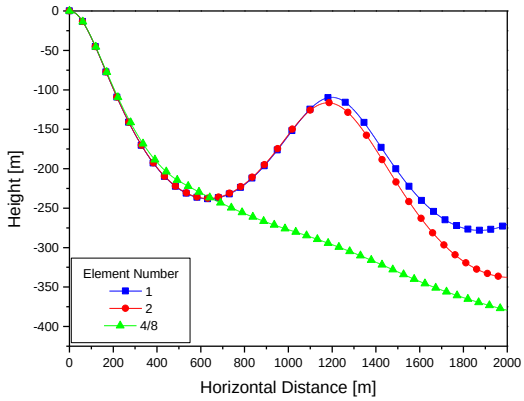

Figure 9 – 2000m range sub-optimal trajectories

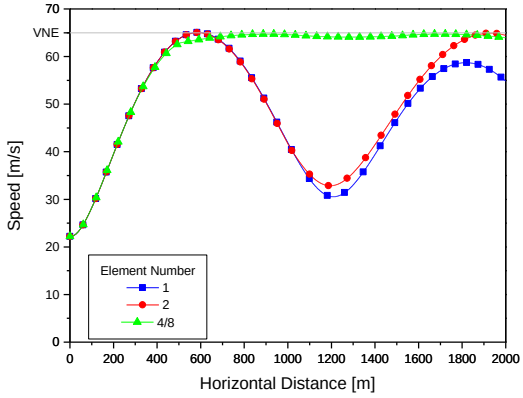

Figure 10 – 2000m range velocity profiles

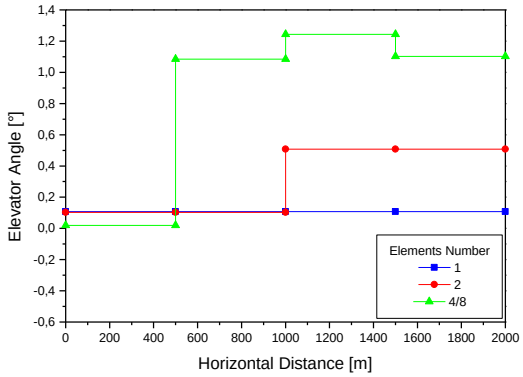

Figure 11 – 2000m range sub-optimal control

Table 5 – 4000m range results

DELTA1 (°)	DELTA2 (°)	DELTA3 (°)	DELTA4 (°)	DELTA5 (°)	DELTA6 (°)	DELTA7 (°)	DELTA8 (°)	TIME (SEC)
.1305	-	-	-	-	-	-	-	93.85
.1352	.9495	-	-	-	-	-	-	84.01
.1198	.5262	1.1884	1.0821	-	-	-	-	79.67
.0396	1.0367	1.2811	1.0886	1.2592	1.1061	1.2607	1.0821	71.64

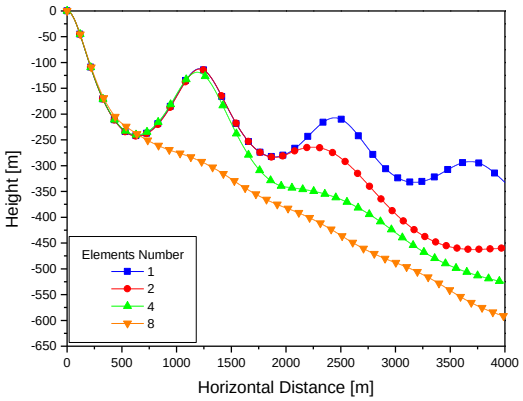

Figure 12 – 4000m range sub-optimal trajectories

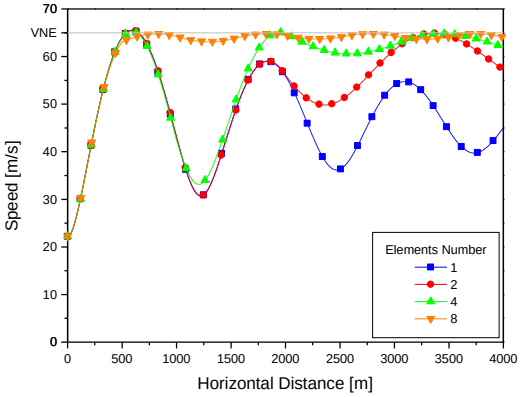

Figure 13 – 4000m range velocity profiles

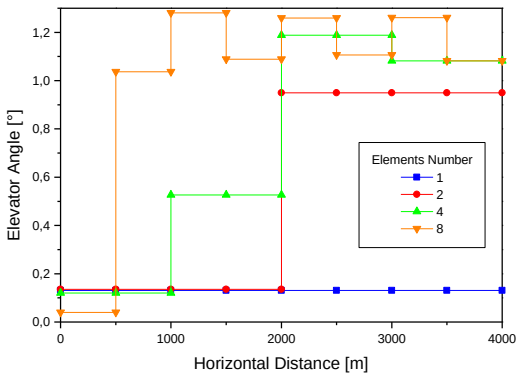

Figure 14 – 2000m range sub-optimal control

ANALYSIS OF RESULTS

Figure 15, Figure 16, and Figure 17 show the overlay of optimal trajectories results for 1000*m*, 2000*m*, and 4000*m* range problems, taking into account the finest discretization.

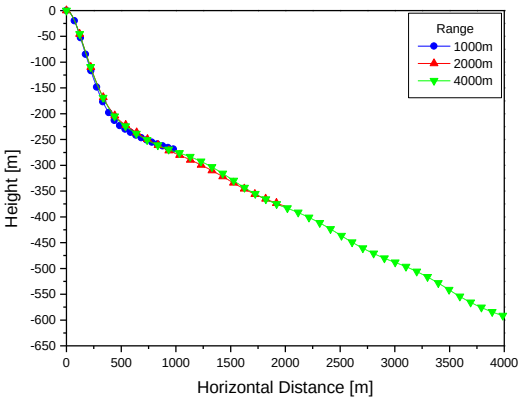

Figure 15 – Optimal trajectories

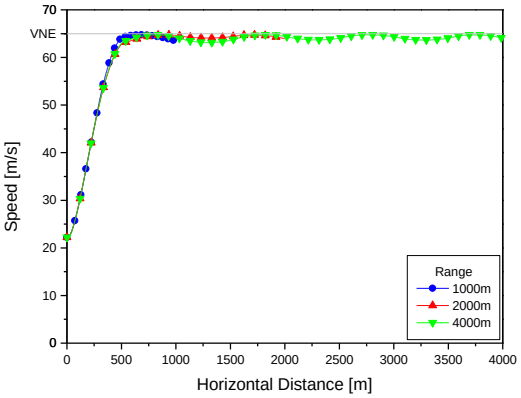

Figure 16 – Optimal Velocity profiles

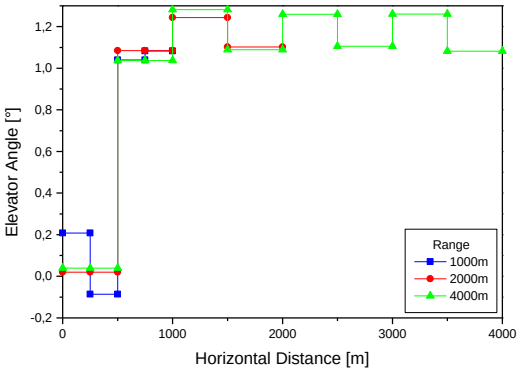

Figure 17 – Optimal controls

COMMENTS

i) Notice that the optimal trajectory has the tendency to reach, as fast as possible, the aircraft velocity limit (*VNE*) and from then, sustain this velocity until the end of flight.

Apparently, the ideal point to reach the VNE is approximately at 500*m* of horizontal displacement.

ii) One must also notice that the obtained sub-optimal trajectory was not firmly established on the *VNE*. The small variation obtained would probably be removed if higher numbers of elements are taken into account and if more precise convergence criteria are adopted.

iii) Tests were performed using a classic non adaptive fourth order *Runge-Kutta Method*. The results do not reached the minimum precision desired, even with a progressive integration step reduction.

CONCLUSION

A dynamic model for sailplane symmetrical motion which takes into account pitch motion, non-linearity on lift curves and air density variations according to height was presented. A procedure to obtain the minimum time trajectories for competition sailplane crossing between thermals was developed. Sub-optimal results were obtained for 1000*m*, 2000*m*, and 4000*m* range trajectories for the sailplane *PIK-20B*.

The obtained results are promising and the authors intend to adopt more elaborate sub-optimal control laws in order to obtain the optimal trajectories for the complete mission.

REFERENCES

De Jong, J.L., 1981, *"The Convex Combination Approach"*, XVII OSTIV Congress, Paderborn, Alemanha, pp. 182-201.

Dickmanns, E.D., 1981, *"Optimal Dolphin Style Soaring"*, XVII OSTIV Congress, Paderborn, Alemanha, pp. 210-212.

Kawabe, H., **Goto,** N., 1994, *"Sailplane Trajectory Optimization"*, Technology Reports of Kyushu University, Vol. 67, n°5 pp. 609-616.

Luenberger, D.G., 1984, *"Linear and Nonlinear Programing"*, Addison-Wesley Publishing Company, London.

Metzger, D.E., **Hedrick,** J. K., 1974, *"Optimal Flight Paths for Soaring Flight"*, American Institute of Aeronautics and Astronautics, pp. 1-7.

Mozdyniewicz, W., 1981, *"Basic Dolphin Tatics"*, XVII OSTIV Congress, Paderborn, Alemanha, pp. 174-181.

Pierson, B.L., **De Jong,** J.L., 1978, *"Cross-Country Sailplane Flight as a DynamicOptimization Problem"*, International Journal for Numerical Methods in Engineering, Vol.12, pp. 1743-1759.

Pinto, R.L.U. de F., 1991, *"Dedução de Condições Necessárias para a Solução de Problemas de Controle Ótimo com Dinâmica Fracionada e Restrições Não-Diferenciadas"*, Tese de Doutorado, Instituto Nacional de Pesquisas Espaciais, São José dos Campos, São Paulo, 190p.

Pinto, R.L.U. de F.., 1982, *"Estudo da Solução de Problemas de Controle Ótimo na forma de Bolza pelo Método dos Elementos Finitos"*, Dissertação de Mestrado, Instituto Tecnológico de Aeronáutica, São José dos Campos, São Paulo, 132p.

Pinto, R.L.U. de F.; **Barros,** C.P.; **Oliveira,** P.H.I.A. de, 1999, *"Um Procedimento Alternativo para Cálculo Aerodinâmico de Aeronaves Leves Subsônicas",* VII Congresso Internacional da Engenharia da Mobilidade, SAE Brasil, São Paulo.

Press, W.H., **Teukolsky,** S.A., **Vetterling,** W.T., **Flannery,** B.P., 1992, *"Numerical Recipes in FORTRAN 77"*, Second Edition, Cambridge University Press, Cambridge, USA.

Reichman, H., 1978, "*Cross-Country Soaring (Streckensegelflug)"*, Thomson Publications, Santa Monica, Califórnia, EUA, 151p.

Vanderbei, R.J., 2000, *"Case Studies in Trajectory Optimization: Trains, Planes and Others Pastimes"*, Princeton University, 29p.

Weinholtz, F.W., 1967, "*Teoria Básica do Moderno Vôo de Distância em Planadores*", Associação Brasileira de Vôo a Vela, São Paulo, Brasil, 96p.